

# Self-Propulsion of Droplets by Spatially-Varying Roughness

Zhenwei Yao and Mark J. Bowick  
 Physics Department, Syracuse University, Syracuse, New York 13244-1130, USA

Under partial wetting conditions, making a substrate uniformly rougher enhances the wetting characteristics of the corresponding smooth substrate – hydrophilic systems become even more hydrophilic and hydrophobic systems even more hydrophobic. Here we show that spatial texturing of the roughness may lead to spontaneous propulsion of droplets. Individual droplets are driven toward regions of maximal roughness for intrinsically hydrophilic systems and toward regions of minimal roughness for intrinsically hydrophobic systems. Spatial texturing can be achieved by wrinkling the substrate with sinusoidal grooves whose wavelength varies in one direction (inhomogeneous wrinkling) or lithographically etching a radial pattern of fractal (Koch curve) grooves on the substrate. Richer energy landscapes for droplet trajectories can be designed by combining roughness texturing with chemical or material patterning of the substrate.

PACS numbers: 47.55.dr, 68.08.Bc

Consider a liquid droplet partially wetting a solid substrate such as glass in contact with a gas such as air. Broadly speaking a substrate may wet easily (hydrophilic) or poorly (hydrophobic) depending on the nature of the substrate, the liquid and the gas. More specifically the three relevant interfacial surface tensions determine the contact angle made by the liquid-gas contact line meeting the plane of the substrate. The contact angle is less than  $90^\circ$  for hydrophilic systems and greater than  $90^\circ$  for hydrophobic systems. A totally wetting thin film corresponds to vanishing contact angle and a complete spherical drop balanced at a point on the substrate corresponds to the superhydrophobic limit with a  $180^\circ$  contact angle.

Uniform surface roughness amplifies the basic wetting characteristics of the corresponding planar system. For hydrophilic/hydrophobic systems the greater substrate area, for a given planar projection, available on the rough substrate makes the wetting more/less favorable and lowers.raises the contact angle. What about surfaces with spatially inhomogeneous properties? Although variable chemical patterning [1] and Leidenfrost droplets contacting hot surfaces with asymmetric sawtooth patterns [2, 3] have been thoroughly explored, this letter addresses the energetic driving forces acting on droplets on a substrate with pure *inhomogeneous* roughness and no other variability. Droplets will spontaneously move around in the landscape of the surface topography maximizing or minimizing the roughness for naturally hydrophilic/hydrophobic systems respectively. Thus self-propelled droplets can be engineered to follow prescribed paths without external drive by appropriately designing the surface topography.

The principle of driving liquid droplets via roughness gradients is simple. The free energy of a liquid droplet on a substrate is  $F = -IA_c + \sigma_{SV}A_t + \sigma_{LV}A_{LV}$ , where  $I = \sigma_{SV} - \sigma_{SL}$  is the imbibition parameter [4],  $\sigma_{SL}$ ,  $\sigma_{SV}$  and  $\sigma_{LV}$  are the respective surface tensions between the three phases (Solid/Liquid/Vapor),  $A_c$  is the contact area between the droplet and substrate,  $A_t$  is the (constant) total area of a substrate and  $A_{LV}$  is the area of the

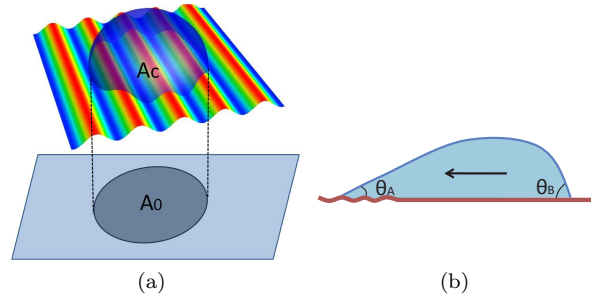


FIG. 1: (a) A liquid droplet sitting on a rough substrate has more contact area with the substrate ( $A_c > A_0$ ) than the same droplet on an otherwise identical flat substrate. (b) A liquid droplet partially wetting a hydrophilic substrate with inhomogeneous roughness has a smaller contact angle at the rougher end ( $\theta_A$ ) than at the smoother end ( $\theta_B$ ).

liquid-vapor interface, which is taken to be constant even when a droplet moves. The system of a liquid droplet on a rough substrate may also be viewed as a droplet on a flat substrate with an effective imbibition parameter  $I_{eff}$  resulting from the roughness.  $I_{eff}$  is defined by  $IA_c \equiv I_{eff}A_0$ , where  $A_0$  is the planar projection of the actual contact area. For rough surfaces,  $A_c > A_0$ , as shown in Fig.1(a), and therefore  $I_{eff}/I > 1$ . Up to irrelevant constants, the free energy of a droplet on a rough substrate is

$$F = -I_{eff}(\vec{x})A_0, \quad (1)$$

where  $I_{eff}$  varies from place to place when the spatial roughness is inhomogeneous. The wetting characteristics of a substrate/liquid composite system determines the sign of  $I$  and therefore  $I_{eff}$ . A hydrophilic system is characterized by  $I > 0$  and an acute contact angle  $\theta = \arccos(I/\sigma_{LV})$ . A hydrophobic system is characterized by  $I < 0$  and an obtuse contact angle [4]. When  $I$ , and so  $I_{eff}$ , is positive (negative) a substrate lowers (increases) its free energy when covered by a liquid. This spontaneously drives droplets on hydrophilic (hydrophobic) substrates towards rougher (smoother) regions re-

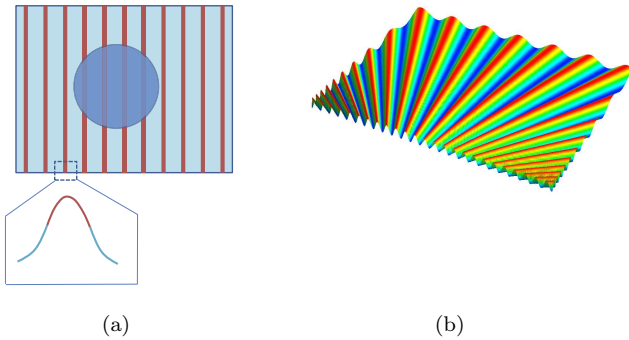


FIG. 2: (a) A liquid droplet partially wetting a substrate with a uniaxial sinusoidally modulated roughness. (b) Schematic plot of sinusoidal grooves with wavenumber monotonically increasing in the direction orthogonal to the sinusoidal height profile.

spectively. Eq.(1) can also be used to understand the movement of droplets on a chemically heterogeneous substrates where  $I_{eff}(\vec{x})$  depends on the wetting characteristics of the chemical composition at the corresponding position on the substrate.

The self-propulsion of liquid droplets on substrates with inhomogeneous roughness can also be understood in terms of the uneven distribution of the Laplace pressure across the droplet. The contact angle for a rough substrate ( $\theta_r$ ) is given by  $\cos \theta_r = r \cos \theta$ , with  $r = A_c/A_0$  [5]. Thus surface roughness amplifies the intrinsic wetting properties of the corresponding planar substrate. Take a droplet spanning a hydrophilic surface that is rougher on the left than on the right, as illustrated in Fig.1 (b). The contact angle is then smaller on the left than on the right:  $\theta_A < \theta_B$ . The mean curvature  $H$  at the B end thus exceeds that at the A end, leading to a Laplace over-pressure ( $P = 2\sigma_{LV}H$ ) gradient from right to left driving the droplet to the rougher part of the surface. The reverse argument applies to a hydrophobic substrate, leading to motion towards the smoother part of the substrate. The self-propulsion of a droplet on a substrate with spatially varying roughness clearly requires the size of the contact disk between the droplet and the substrate to be larger than the typical size over which the roughness varies significantly.

To be specific, consider a droplet on a uniaxial sinusoidal substrate, as shown in Fig.2(a), realizable via wrinkled membranes [6]. The height of the substrate is represented by  $z(x) = a_k \cos(kx)$ , with translational invariance along the y-direction. The roughness amplitude  $a_k$  will be taken much smaller than the maximum height of the droplet so that the shape of the liquid-air interface is unaffected by the shape of the substrate. For small amplitude roughness liquid droplets can be in complete contact with the substrate, since air pockets do not form underneath the liquid [4, 5]. The effective imbibition pa-

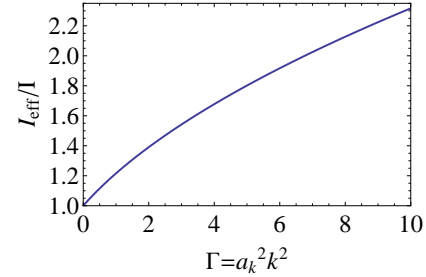


FIG. 3: The ratio of the effective imbibition parameter to the physical imbibition parameter versus  $\Gamma = a_k^2 k^2$  for a liquid droplet partially wetting a sinusoidally modulated substrate.

rameter is given by

$$\frac{I_{eff}}{I} = \frac{4}{\pi} \int_0^1 dy \sqrt{1 - y^2} \sqrt{1 + \Gamma \sin^2(\tilde{k}y)}, \quad (2)$$

where  $\tilde{k} = kR$  is the dimensionless wavenumber and  $\Gamma = a_k^2 k^2$ . Clearly  $\Gamma$ , arising from the gradient of the substrate height, is the parameter controlling the effective imbibition. For  $R >> \frac{2\pi}{k}$ , Eq.(2) simplifies to [7]

$$\frac{I_{eff}}{I} = \frac{2}{\pi} R(\Gamma), \quad (3)$$

where  $R(x) = \int_0^{\pi/2} d\theta \sqrt{1 + x \sin^2 \theta}$ . In this limit the effective imbibition parameter is dependent only on the product of the amplitude and the wavenumber of the sinusoidal substrate. Fig.3 is a numerical plot of the monotonic growth of  $I_{eff}/I$  vs.  $\Gamma$ .  $I_{eff}/I$  is doubled for  $\Gamma \approx 8$ . A simple gradient of the effective imbibition parameter over the substrate can be achieved by varying the wavenumber  $k$  along the groove axis (y), as shown in the schematic Fig.2(b). Droplets will migrate to maximize/minimize the contact area for intrinsically hydrophilic/hydrophobic substrates. The magnitude of the driving force along the groove axis is proportional to the gradient of the effective imbibition parameter:

$$\nabla_y I_{eff} = \frac{2I}{\pi} [R(\Gamma) - S(\Gamma)] \frac{d \ln \tilde{k}(y)}{dy}, \quad (4)$$

where  $S(x) = \int_0^{\pi/2} \frac{d\theta}{\sqrt{1+x \sin^2 \theta}}$ , and  $R(x) - S(x) = \frac{\pi x}{4} - \frac{3\pi x^2}{32} + \mathcal{O}(x^3)$ . The driving force thus depends rather weakly on  $\tilde{k}(y)$  and vanishes as  $\Gamma$  approaches zero.

Rough substrates may also be designed based on fractals [8]. Consider a substrate with etched grooves whose cross section is the lower half of the Koch curve, as illustrated in Fig.4 [9]. The Koch curve may be constructed by starting with an equilateral triangle of side length  $a_0$  and perimeter  $L_0 = 3a_0$ , then recursively adding equilateral triangles symmetrically on each line segment. After  $n$  steps, the perimeter of the new graph becomes  $L_n = L_0(4/3)^n$  with the length of each elementary line segment being  $a_n = a_0(1/3)^n$ . The Hausdorff, or self-similarity, dimension of the Koch curve is

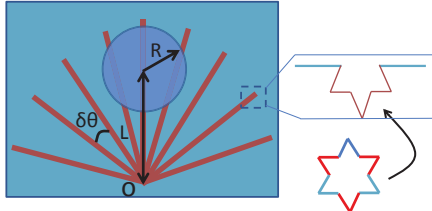


FIG. 4: A substrate etched by fractal grooves. The cross-sectional shape of the grooves is the lower half of the Koch curve, as shown in the inset.

$d_H = \ln 4 / \ln 3 \approx 1.26$  [10]. Now consider a set of close-packed evenly aligned straight grooves constructed from an  $n$ -th order Koch curve. The distance between two neighboring grooves is twice the breadth of a groove. The contact area between a droplet of radius  $R$  and the fractal substrate, in the limit  $R$  much bigger than the breadth of a groove, is  $A_c = \pi R^2 [1 + q(n)]$ , where  $q(n=0) = 3/4$  and  $q(n > 0) = 2(4/3)^{n-2} - 1/2$ . Since  $q(n)$  is always positive,  $A_c/A_0 > 1$ . The effective imbibition parameter is

$$\frac{I_{eff}}{I} = 1 + q(n). \quad (5)$$

Thus the effective imbibition parameter depends only on the order of the Koch curve  $n$  and is independent of the seed side length  $a_0$ .  $I_{eff}/I$  is two for  $n = 1$  and exceeds 10 for  $n = 8$ . Note that the extra volume of liquid inside the finer structure of the fractal grooves is negligible in the limit of large  $n$  as the area  $A_n$  of the  $n$ -th order Koch curve converges:  $\lim_{n \rightarrow \infty} A_n = 2\sqrt{3}a_0^2/5 \sim a_0^2 \ll a_0 h$ , where  $h$  is the droplet thickness.

An effective roughness gradient can be made by etching a radial array of grooves with Koch cross-section, as sketched in Fig.4. We take an intrinsically hydrophobic surface inclined at an angle  $\alpha$  to the horizontal. A droplet sitting near the origin (O) of the radial array will move upward to reduce the contact energy provided the gradient of the effective imbibition parameter is sufficient to overcome gravity. The number of grooves covered by a droplet of size  $R$  is  $N = 2R/(L\delta\theta)$ , where  $\delta\theta$  is the angular distance between neighboring grooves and  $L$  is the distance of the droplet from the origin. For simplicity, consider the “far-field” limit in which the droplet is sufficiently far from the origin that all the grooves under the droplet are effectively parallel. The change in contact area due to the roughness is  $\Delta A = A_c - A_0 = \frac{1}{2}N\pi(b_n - l_0)R$ , where  $b_n$  is the area of a groove of unit length with  $b_n(n > 0) = \frac{3a_0}{2}(\frac{4}{3})^n$  and  $b_n(n = 0) = 5a_0/3$ , and  $l_0 = 2a_0/3$  is the groove breadth. This results in an effective imbibition parameter

$$\frac{I_{eff}}{I} = 1 + \frac{b_n - l_0}{L\delta\theta}. \quad (6)$$

A droplet rising up a distance  $\delta L$  increases its gravitational potential energy by  $\delta W = mg\delta L \sin \alpha$ , where  $m \sim \rho R^2 h$  is the mass of the droplet. Meanwhile the surface energy decreases by  $\delta F = A_0\delta I_{eff}$ , where  $\delta I_{eff} = I_{eff}(L+\delta L) - I_{eff}(L)$ . Spontaneous climb therefore requires  $\delta I_{eff}/\delta L > mg \sin \alpha / A_0$ . Inserting Eq.(6) for the effective imbibition parameter yields

$$\frac{b_n - l_0}{l_0} > \frac{L^2 \delta\theta \ mg \sin \alpha}{A_0 I l_0}. \quad (7)$$

This condition can be satisfied for large droplets near the origin on substrates with dense grooves. The right hand side of Eq.(7) is of order  $10 \sin \alpha$  for  $L \sim \text{cm}$ ,  $R \sim \text{mm}$ ,  $I \sim \text{mN/m}$ ,  $\delta\theta \sim a_0/L$  and  $h \sim 0.1R$ . Since  $(b_n - l_0)/l_0 \sim 10$  for  $n = 5$ , radially carved grooves made of the 5-th order Koch curves would generate sufficient roughness gradient to drive droplets uphill.

There are several points in our analysis that may ultimately call for a more thorough treatment. Sharp substrate edges impede the motion of droplets via pinning of the triple line [11]. Adhesion hysteresis may also arise from the microscopic interactions between a droplet and the substrate [12]. These two effects are the main source of frictional energy dissipation [13]. We have neglected entirely viscous dissipation due to internal fluid flow within moving droplets [4, 14].

Droplet flow driven by inhomogeneous surface roughness is strictly downhill according to the gradient of the height profile of the surface but one may also vary the chemical composition of the surface so that the intrinsic surface tensions are spatially dependent. The combination of chemical and roughness patterning offers a rich variety of potential structures to obtain desired flow patterns. The African beetle *Stenocara* fog-bisks by tilting forward into the early morning fog-laden wind of the Namib desert and collecting micron-sized water droplets on the smooth hydrophilic peaks of its fused overwings (elytra) [15]. Once a sufficiently massive droplet is formed it rolls downhill against the wind to pool in textured hydrophobic waxy troughs and from there to the beetle’s mouth. Surface structures modeled on the *Stenocara* wings have been synthesized by creating hydrophilic patterns on superhydrophobic surfaces with water/2-propanol solutions of a polyelectrolyte [16].

This work was supported by the National Science Foundation grant DMR-0808812 and by funds from Syracuse University. We are grateful for productive discussions with Cristina Marchetti, Pat Mather, Shiladitya Banerjee and Pine Yang.

[1] F. Brochard, Langmuir **5**, 432 (1989).

[2] D. Quéré and A. Ajdari, Nat. Mater. **5**, 429 (2006).

[3] H. Linke *et al.*, Phys. Rev. Lett. **96**, 154502 (2006).

[4] P.G. de Gennes, F. Brochard-Wyart, and D. Quéré, *Cap-*

- illarity and Wetting Phenomena: Drops, Bubbles, Pearls, Waves* (Springer, New York, 2003).
- [5] R.N. Wenzel, Ind. Eng. Chem. **28**, 988 (1936).
- [6] D. Vella, M. Adda-Bedia and E. Cerdà, Soft Matter **6**, 5778 (2010).
- [7] The contact area  $A_c$  of a droplet of radius  $R$  and a sinusoidal substrate can be calculated in the Cartesian coordinates with the origin at the center of the droplet. The contact area in the first quadrant is  $A_c/4 = \sum_{i=0}^{N=R/\lambda} L_\lambda \sqrt{R^2 - x_i^2}$ , where  $x_i = i\lambda$  ( $i = 0, 1, 2..N$ ) are the positions of the sinusoidal peaks. For  $R >> \lambda$ ,  $\sum_{i=0}^{N=R/\lambda} \Delta i = \int_0^N di$ , where  $\Delta i = 1$ .  $A_c$  can thus be obtained by integration.
- [8] T. Onda, S. Shibuichi, N. Satoh and K. Tsujii, Langmuir **12**, 2125 (1996).
- [9] H. von Koch, Acta Math. **30**, 145 (1906).
- [10] K. Falconer, *Fractal Geometry: Mathematical Foundations and Applications* (Wiley, New Jersey, 1990).
- [11] M. Nosonovsky and B. Bhushan, Microsyst. Technol. **11**, 535 (2002).
- [12] *Nanotribology and Nanomechanics: An Introduction*, edited by B. Bhushan (Springer, New York, 2005).
- [13] M. Nosonovsky, J. Chem. Phys. **126**, 224701 (2007).
- [14] L.D. Landau and E.M. Lifshitz, *Fluid Mechanics*, 2nd edition (Pergamon Press, Oxford, 1987).
- [15] A. R. Parker and C.R. Lawrence, Nature **414**, 33 (2001).
- [16] L. Zhai *et al.*, Nano Lett. **6**, 1213 (2006).